Preclinical Evaluation of a Modified Herpes Simplex Virus Type 1 Vector Encoding Human TGM1 for the Treatment of Autosomal Recessive Congenital Ichthyosis

John C. Freedman[1], Trevor J. Parry[1], Peipei Zhang[1], Avijit Majumdar[1], Suma Krishnan[1], Lauren K. Regula[1], Mark O'Malley[1], Sarah Coghlan[1], S.D. Yogesha[1], Sureshkumar Ramasamy[1] and Pooja Agarwal[1]

Autosomal recessive congenital ichthyosis (ARCI) is a diverse group of cornification diseases associated with severe clinical complications and decreased quality of life. Germline mutations in the *TGM1* gene, which encodes the enzyme TGM1, are the predominant cause of ARCI. These *TGM1* mutations trigger the abnormal epidermal differentiation and impaired cutaneous barrier function observed in patients with ARCI. Unfortunately, current ARCI therapies focus solely on symptomatic relief. Thus, there is a significant unmet need for therapeutic strategies aimed at correcting the TGM1 deficiency underlying ARCI. In this study, we investigated the ability of KB105, a gene therapy vector encoding full-length human *TGM1*, to deliver functional human TGM1 to keratinocytes. In vitro, KB105 efficiently infected TGM1-deficient human keratinocytes, produced TGM1 protein, and rescued transglutaminase enzyme function. In vivo studies demonstrated that both single and repeated topical KB105 administration induced TGM1 protein expression in the target epidermal layer without triggering fibrosis, necrosis, or acute inflammation. Toxicity and biodistribution assessments on repeat dosing indicated that KB105 was well-tolerated and restricted to the dose site. Overall, our results demonstrate that rescuing TGM1 deficiency in patients with ARCI through topical KB105 application represents a promising strategy for safely and noninvasively treating this debilitating disease.

Journal of Investigative Dermatology (2021) **141,** 874–882; doi:10.1016/j.jid.2020.07.035

INTRODUCTION

Autosomal recessive congenital ichthyosis (ARCI) is a heterogeneous group of rare cornification diseases affecting approximately 1:200,000 persons (Orphanet, 2020). Whereas pathogenic mutations in at least 12 genes have been identified in patients with ARCI, germline mutations in the *TGM1* gene affect >55% of those with ARCI in the United States (Rodríguez-Pazos et al., 2013) and up to 84% of ARCI cases in Norway (Farasat et al., 2009; Pigg et al., 1998).

TGM1 is an intracellular enzyme that plays a critical role in the formation of the cornified envelope (CE), a structure that acts as a mechanical barrier against transepidermal water loss and entry of infectious agents. TGM1 is mainly localized within the stratum granulosum, stratum corneum, and hair follicles, where it catalyzes the covalent cross-linking of different CE proteins (Candi et al., 2005). Loss of TGM1 activity compromises the CE and leads to abnormal barrier function, initiating a default compensatory pathway of hyperproliferation resulting in a clinical presentation of localized and/or generalized scaling (Yang et al., 2016). Disruptive *TGM1* gene mutations lead to the chronic and often devastating abnormal epidermal differentiation and defective cutaneous barrier function observed in patients with ARCI (Herman et al., 2009).

Individuals with TGM1-associated ARCI are typically born encased in a tight, shiny collodion membrane, which sheds during the first weeks of life. Neonatal complications occur in 45% of cases, leading to an infant mortality rate of ~11% (Chung et al., 2011). After the shedding of the collodion membrane, plate-like scales develop on the skin and usually affect the entire integument. Other signs and symptoms include a predisposition to heat intolerance, eclabium and ectropion, hair loss, palmoplantar hyperkeratosis, nail abnormalities, conductive hearing loss, and respiratory problems. Quality of life is negatively impacted from a young age, resulting in life-long social stigmatization, shyness, and up to 4 hours of skin care daily (Gånemo et al., 2003).

Unfortunately, current therapeutic options for treating ARCI provide only symptomatic relief. For those with severe skin involvement, retinoid therapy is often prescribed; however, retinoids fail to restore epidermal barrier function and carry the potential for significant complications. There is a substantial unmet need for a therapy that molecularly corrects the TGM1 deficiency underlying ARCI.

[1]*Krystal Biotech, Inc, Pittsburgh, Pennsylvania, USA*

Correspondence: Suma Krishnan, Krystal Biotech, Inc, 2100 Wharton Street, Suite 701, Pittsburgh, Pennsylvania, USA 15203. E-mail: skrishnan@krystalbio.com

Abbreviations: ARCI, autosomal recessive congenital ichthyosis; CE, cornified envelope; IF, immunofluorescence; KC, keratinocyte; MOI, multiplicity of infection

Received 7 February 2020; revised 14 July 2020; accepted 16 July 2020; accepted manuscript published online 22 September 2020; corrected proof published online 10 February 2021

In this study, we investigate the TGM1-modifying effects of KB105, a replication-defective herpes simplex virus type 1 gene therapy vector encoding full-length human *TGM1*. In vitro, we demonstrate that KB105 efficiently infects relevant TGM1-deficient human skin cells and rescues transglutaminase enzyme function. In vivo, KB105 yields significant TGM1 protein expression without toxicity when applied topically to immunocompetent animals. In the epidermis, topical readministration of KB105 sustains high *TGM1* DNA and RNA levels while simultaneously boosting TGM1 protein levels. Finally, evaluation of vector toxicity and biodistribution on weekly redosing indicates that KB105 is well-tolerated and remains limited to the dose site. Taken together, these preclinical proof-of-concept studies and safety assessments provide strong support for the recurrent use of topical KB105 as a safe and effective treatment for TGM1-deficient ARCI.

RESULTS

KB105 pharmacology in immortalized TGM1-deficient patient-derived keratinocytes

Purified KB105 was first evaluated for transduction efficiency and effector expression in two-dimensional cell-based assays. These assays employed immortalized human keratinocytes (KCs) harvested from a patient with TGM1-deficient ARCI homozygous for a c.877-2A>G splice-site mutation, the most commonly reported *TGM1* mutation in humans (Herman et al., 2009). Cells were infected with KB105 at multiplicities of infections (MOIs) ranging from 0.3 to 3.0 for 48 hours, and vector transduction and effector expression were analyzed by qPCR, quantitative real-time RT-PCR, western blot, and immunofluorescence (IF). Negative controls included uninfected cells (mock) and cells infected with an mCherry-expressing vector (mCherry).

KB105 vector genomes and *TGM1* transcript expression were detected in patients with TGM1-deficient ARCI-derived KCs at an MOI as low as 0.3 and showed a dose-dependent increase in *TGM1* DNA (Figure 1a) and RNA (Figure 1b) levels. Increased TGM1 protein expression was observed by western blot and immunofluorescent analysis relative to mock-infected controls (Figure 1c and d). No detectable endogenous TGM1 was observed in the uninfected immortalized KCs, confirming that these cells were isolated from a patient harboring a natural TGM1 deficiency.

The functionality of the KB105-expressed human TGM1 was next examined by determining whether the exogenous protein catalyzed covalent cross-linking between glutamine and lysine residues, a function essential for TGM1-mediated assembly of the CE. Protein functionality was assessed using an in situ TGM1-specific peptide cross-linking activity assay employing a biotinylated peptide that mimics a natural TGM1 substrate. TGM1-mediated conjugation of biotinylated peptides was visualized by incubating the treated cells with fluorescently labeled streptavidin. A dose-dependent increase in TGM1 enzymatic activity was observed in KB105-infected cells by IF, with TGM1-mediated peptide cross-linking in infected cells surpassing the levels of endogenous TGM1 activity in normal primary KCs (Figure 1e). Uninfected (mock) cells showed no detectable TGM1 activity. A similar trend in TGM1 protein expression and subsequent restoration of functional activity were observed in immortalized ARCI KCs grown in high calcium medium to stimulate cell differentiation (Supplementary Figure S1a and b).

KB105-mediated TGM1 protein expression in primary human cells

The ability of KB105 to transduce a more clinically relevant cell type, that is, primary TGM1-deficient patient KCs, was next examined. Restoration of TGM1 protein expression was observed by western blot analysis in the KB105-infected primary patient cells (Figure 1f). As expected, no endogenous TGM1 was observed in the negative control primary ARCI KCs. Supporting the western blot, IF data revealed a dose-dependent increase in TGM1 protein between an MOI of 0.3 and 1.0 (Figure 1g). A rescue of TGM1 protein expression in primary patient KCs was also observed by IF after growth in high-calcium cell culture medium (Supplementary Figure S2). No significant impact on cell morphology was observed on KB105 transduction in low or high calcium environments (Supplementary Figure S3a). Mild cytotoxic effects were observed at high dosages of the vector in primary cells, which may account for the decreased TGM1 protein levels observed at an MOI of 3 in the western blot and analyses (Supplementary Figure S3b).

In vivo evaluation of KB105 through multiple routes of topical delivery

Because the homozygous deletion of *TGM1* is neonatally lethal in mice (Matsuki et al., 1998), a mouse model harboring a genetic lesion in endogenous *TGM1* was not practicable for preclinical evaluations. As such, in vivo pharmacology of KB105 was conducted in immunocompetent BALB/c mice. This approach allowed the determination of the vector's ability to deliver properly localized TGM1 after single or repeated topical administration while concurrently monitoring the vector's toxicity within a fully intact immune system.

First, an evaluation of KB105 was conducted in mechanically or chemically disrupted dorsal skin of treated mice. Sequential tape stripping and wiping of the skin surface with acetone are the commonly used techniques for skin barrier disruption (Rissmann et al., 2009). A single low or high KB105 dose formulated in a methylcellulose gel carrier was topically administered to two regions of the prepared skin on each mouse. Skin biopsies were harvested 48 hours after topical administration and processed for analysis.

A histological examination of skin samples harvested from each treatment group was conducted to evaluate KB105-induced physiological changes, which may indicate potential safety concerns in vivo. No obvious signs of fibrosis, necrosis, or acute inflammation were detected in any KB105-treated samples compared with vehicle control (Figure 2a). Post-killing qPCR analysis of the topically treated skin indicated that KB105 effectively transduced both the acetone-treated− and tape strip−permeabilized skin (Figure 2b), and high levels of human *TGM1* transcripts were expressed after infection (Figure 2c). Whereas acetone treatment or tape stripping of the skin was found to induce endogenous mouse *TGM1* transcription, no significant differences in endogenous *TGM1* expression were

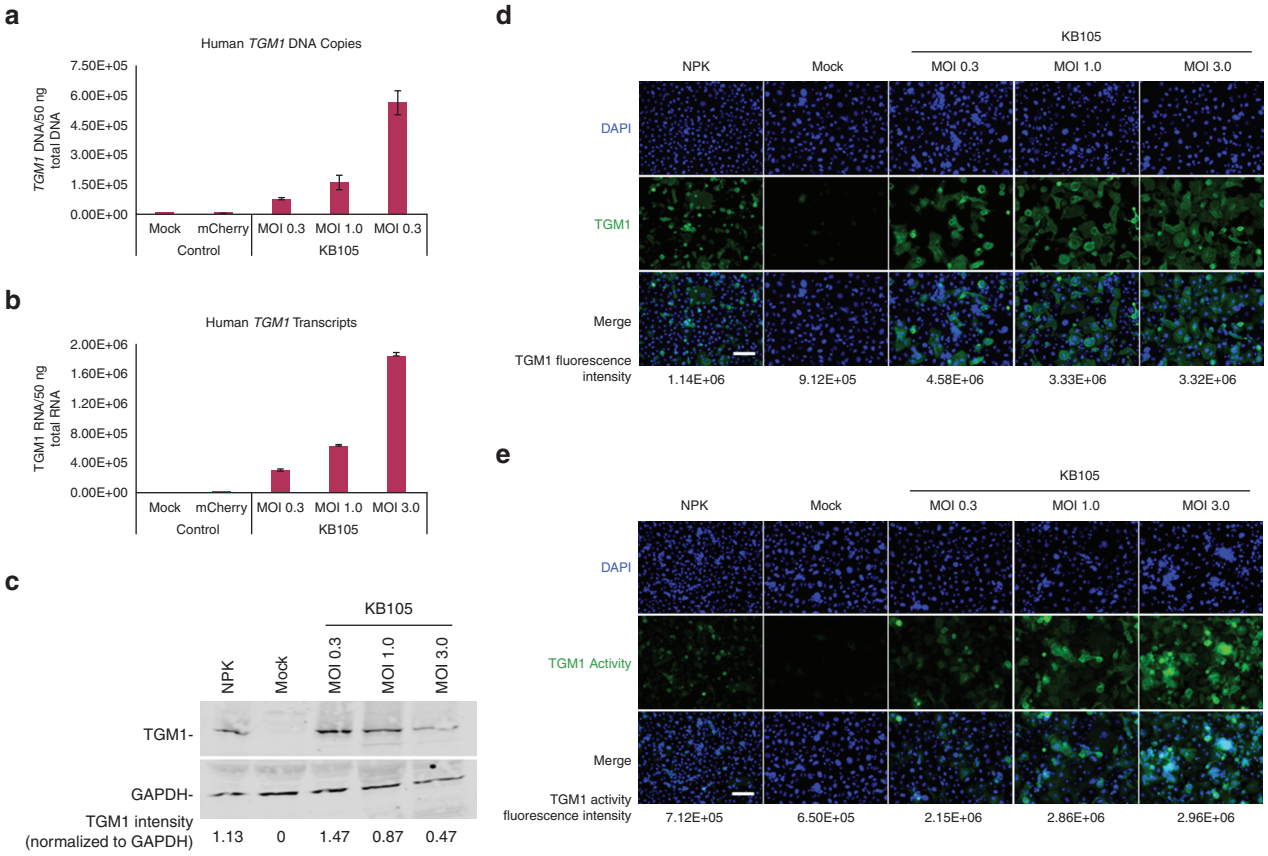

Figure 1. In vitro assessment of KB105 in immortalized and primary TGM1-deficient human ARCI KCs grown in a low-calcium cell culture medium. (**a**) Dose-dependent detection of human *TGM1* DNA copies at increasing MOIs of KB105 in immortalized KCs, as assessed by qPCR. Data are presented as the average of two replicates ± SEM. (**b**) Dose-dependent expression of human *TGM1* transcripts at increasing MOIs of KB105 in immortalized KCs, as assessed by QRT-PCR. Data are presented as the average of two replicates ± SEM. (**c**) KB105-mediated TGM1 protein expression in infected immortalized KCs by western blot. (**d**) Representative IF images of human TGM1 protein expression on KB105 infection of immortalized KCs. (**e**) Representative IF images of KB105-dependent TGM1 enzymatic activity in immortalized KCs. (**f**) KB105-mediated TGM1 protein expression in infected primary cells by western blot analysis. (**g**) Representative IF images of human TGM1 protein expression on KB105 infection of primary cells. For these experiments, uninfected (mock) and HSV-mCherry–infected (mCherry) cells were used as negative controls; NPKs were used as a positive control. DAPI staining was used to visualize the nuclei. GAPDH was used as a loading control. For western blot and IF analyses, quantification of protein levels and fluorescence intensities are provided for each condition. Bar = 130 μm. ARCI, autosomal recessive congenital ichthyosis; HSV, herpes simplex virus; IF, immunofluorescence; KC, keratinocyte; MOI, multiplicity of infection; NPK, normal primary KC; QRT-PCR, quantitative real-time RT-PCR.

observed between low- or high-dose KB105 and vehicle control (Supplementary Figure S4).

Exogenous TGM1 protein expression and tissue localization were assessed by IF. Human TGM1 was detected in mouse epidermis on topical application of KB105 (Figure 2d). Paralleling the qPCR and quantitative real-time RT-PCR results, a qualitative increase in TGM1 protein was observed in the high- versus low-dose samples. Samples were also costained for mouse loricrin (a natural substrate for TGM1) and mouse integrin alpha-6 (a marker of the basal layer of the epidermis) to determine whether the exogenously expressed TGM1, originating from KB105, was correctly localized to the stratum granulosum, the tissue layer where endogenous TGM1 is expressed and functionally active. Mouse loricrin colocalized with human TGM1 in all the KB105-treated samples, whereas TGM1 was detected in a more superficial layer than in mouse integrin alpha-6. Together, these data demonstrate that KB105 successfully transduced the targeted epidermal layer.

A short-term pharmacokinetics study was conducted in the tape-stripped skin of BALB/c mice after topical administration of KB105 (Supplementary Figure S5). Vector genomes in the transduced cells remained relatively stable over the course of the 48-hour study, indicated by similar numbers of human *TGM1* DNA copies between the 8- and 48-hour timepoints. Human *TGM1* transcripts were detected as early as 2 hours after topical application and steadily increased over time, peaking at 24 hours after treatment before declining (while remaining detectable) at 48 hours. Similar transgene kinetics were observed at the protein level, as assessed by IF.

Repeated topical delivery of KB105

We next evaluated the safety and feasibility of repeated in vivo vector applications using two different dosing intervals (days 1 and 3 vs. days 1 and 12). Briefly, mice were tape stripped and treated topically with KB105 (or vehicle control) on day 1. Skin tissues from the first cohort of mice were harvested on day 3 to act as positive (KB105) and

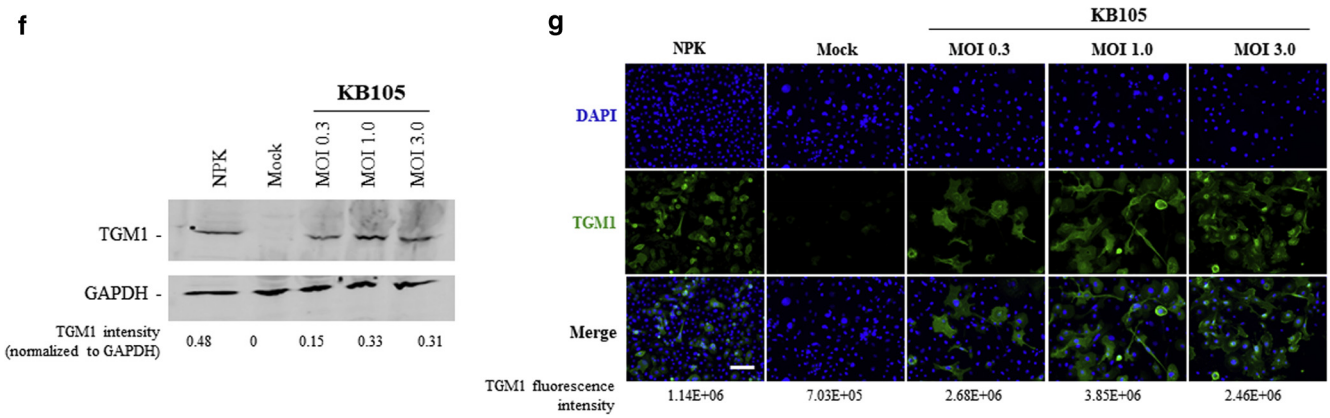

Figure 1. (*Continued*)

negative (vehicle) controls. Additional mice cohorts were re−tape stripped and retreated topically with KB105 on days 3 and 12, with tissues subsequently harvested on days 5 and 14, respectively.

Histological examination of skin samples found no obvious signs of toxicity or tissue reorganization, including fibrosis, necrosis, or acute inflammation, in any of the single or repeat KB105-treated samples (Figure 3a). High vector genome copy numbers were detected at 48 hours after a single administration of KB105; comparable genome copy numbers were also detected at 48 hours after a repeated KB105 dose administered at either day 3 or day

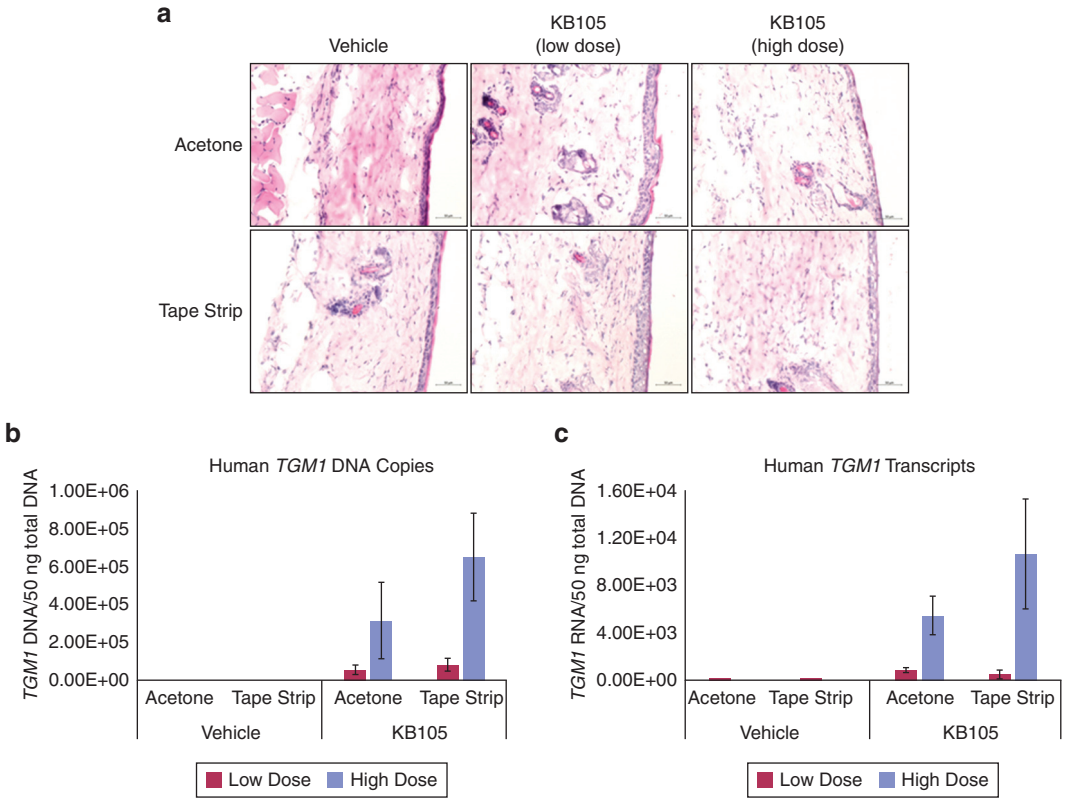

Figure 2. In vivo evaluation of KB105 through multiple routes of topical delivery to BALB/c mice. (**a**) Representative H&E-stained samples harvested from tape-stripped or acetone permeabilized BALB/c mouse skin treated topically with either KB105 (low or high dose) or negative control (vehicle). (**b**) Dose-dependent detection of human *TGM1* DNA copies in mouse skin biopsies harvested at 48 hours after permeabilization by tape stripping or acetone treatment and application of KB105 (low or high dose) or negative control (vehicle), as assessed by qPCR. (**c**) Dose-dependent expression of human *TGM1* transcripts in mouse skin biopsies harvested at 48 hours after permeabilization by tape stripping or acetone treatment and application of KB105 (low or high dose) or negative control (vehicle), as assessed by QRT-PCR. For each vehicle control condition in the qPCR and QRT-PCR analyses, data are presented as the average of two tissue samples (two replicates tested per tissue sample) ± SEM; for each KB105 condition, data are presented as the average of four tissue samples (two replicates tested per tissue sample) ± SEM. (**d**) Representative immunofluorescence images of human TGM1, mouse loricrin, and mouse integrin alpha-6 protein localization in mouse skin biopsies harvested at 48 hours after skin barrier disruption by acetone treatment or tape stripping and application of KB105 (low or high dose) or negative control (vehicle). DAPI staining was used to visualize the nuclei. Bar = 50 μm. QRT-PCR, quantitative RT-PCR.

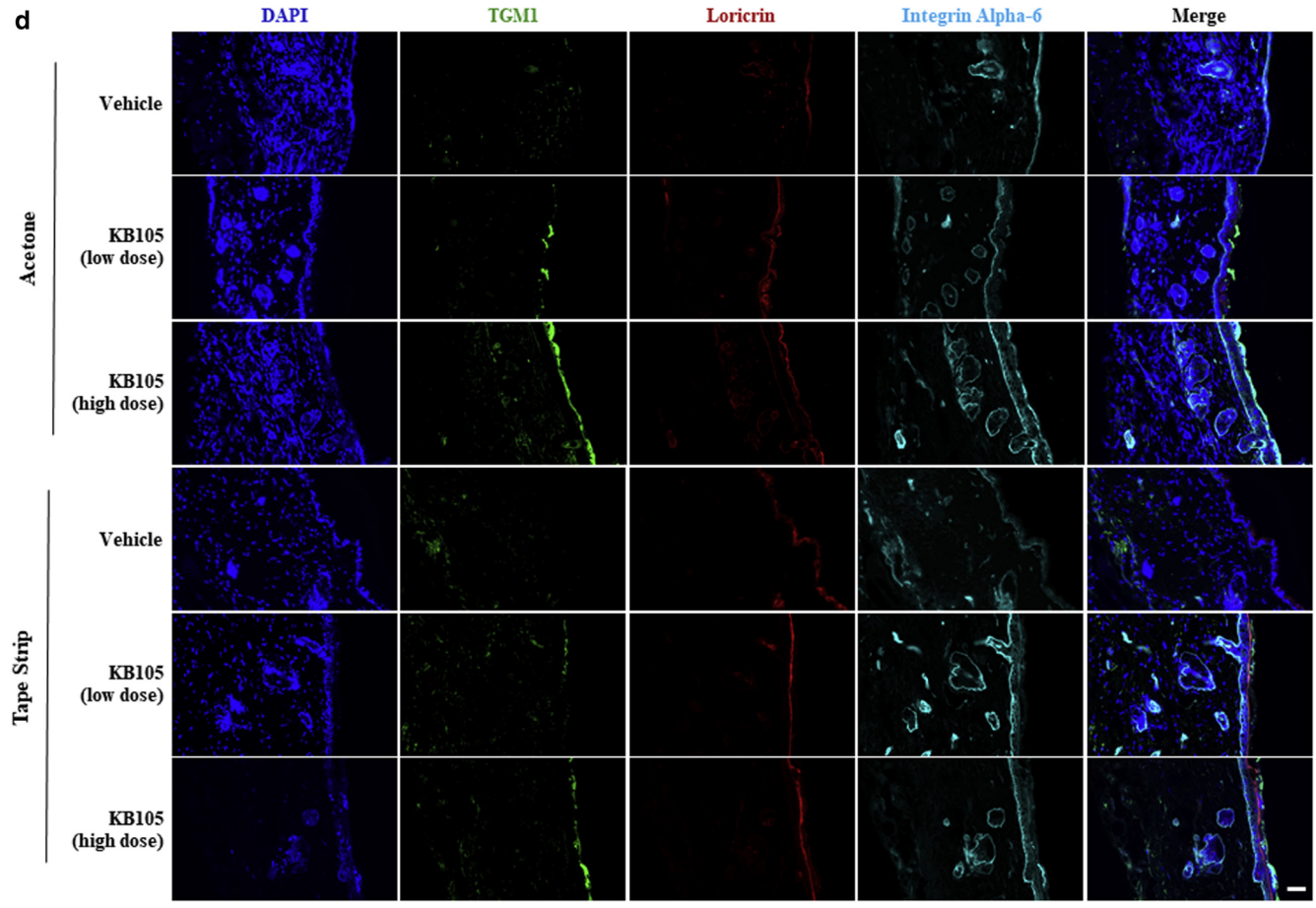

Figure 2. (*Continued*)

12 (Figure 3b). Similar human *TGM1* transcript levels were detected after 48 hours in the mice receiving a single KB105 dose on day 1 or a second dose on days 3 or 12 (Figure 3c).

Human TGM1 protein levels were qualitatively measured. Epidermal localization was assessed by colocalization with mouse loricrin. Significant levels of TGM1 protein as well as proper epidermal localization were detected in the skin tissue biopsies harvested from the mice treated either once or twice with KB105 (Figure 3d). Whereas some variability was observed in *TGM1* transcript numbers in these mouse cohorts, no gross differences in TGM1 protein expression were observed by IF after single versus repeat administration of KB105.

Repeated-dose toxicity and biodistribution of KB105

Toxicity and biodistribution of KB105 were evaluated in a Good Laboratory Practice repeat-dose study in male and female BALB/c mice (Table 1). Mice were dosed once a week for 5 weeks with topical KB105 (group 2) or vehicle control gel (group 1) after skin permeabilization by tape stripping. Six mice per sex per group were administered one dose on day 1 and necropsied on day 3. Six animals per sex per group were dosed on days 1, 8, 15, 22, and 29 and necropsied on day 30. All the remaining surviving mice were dosed on days 1, 8, 15, 22, and 29, and were then subjected to a 33-day recovery phase before necropsy.

Assessment of toxicity was based on mortality, clinical observations, body weights, food consumption, dermal observations, and clinical and anatomic pathology. No KB105-related mortality, clinical observations, body weight or food consumption changes, macroscopic findings, or effects on organ weight parameters were noted. All mice survived until their scheduled necropsy. Microscopic examination was limited to the selected tissues, including application per dose site, sternum with bone, bone marrow, brain, epididymis, heart, kidneys, liver, lungs, axillary lymph node, inguinal lymph node, ovaries, oviducts, prostate, spleen, testes, thymus, and uterus with cervix. Microscopic findings localized to the treated skin site, including hyperkeratosis, epithelial hyperplasia, inflammation, edema, and fibrosis, were evaluated at the interim and terminal killings. These findings were consistent with repair after abrasion and were considered related to the dosing procedure. At the recovery killing, most mice exhibited complete reversibility of the dosing procedure–related microscopic findings. As such, the no observed adverse effect level for topical application of KB105 was found to be 1.07×10^9 plaque-forming unit/day.

Blood and tissue samples were analyzed by qPCR for the determination of KB105 biodistribution. Nearly all the blood and tissue samples collected from the vehicle control mice (group 1) over the three intervals were negative for KB105 except for six dose-site samples. A root cause analysis indicated that a contamination occurred during the preparation

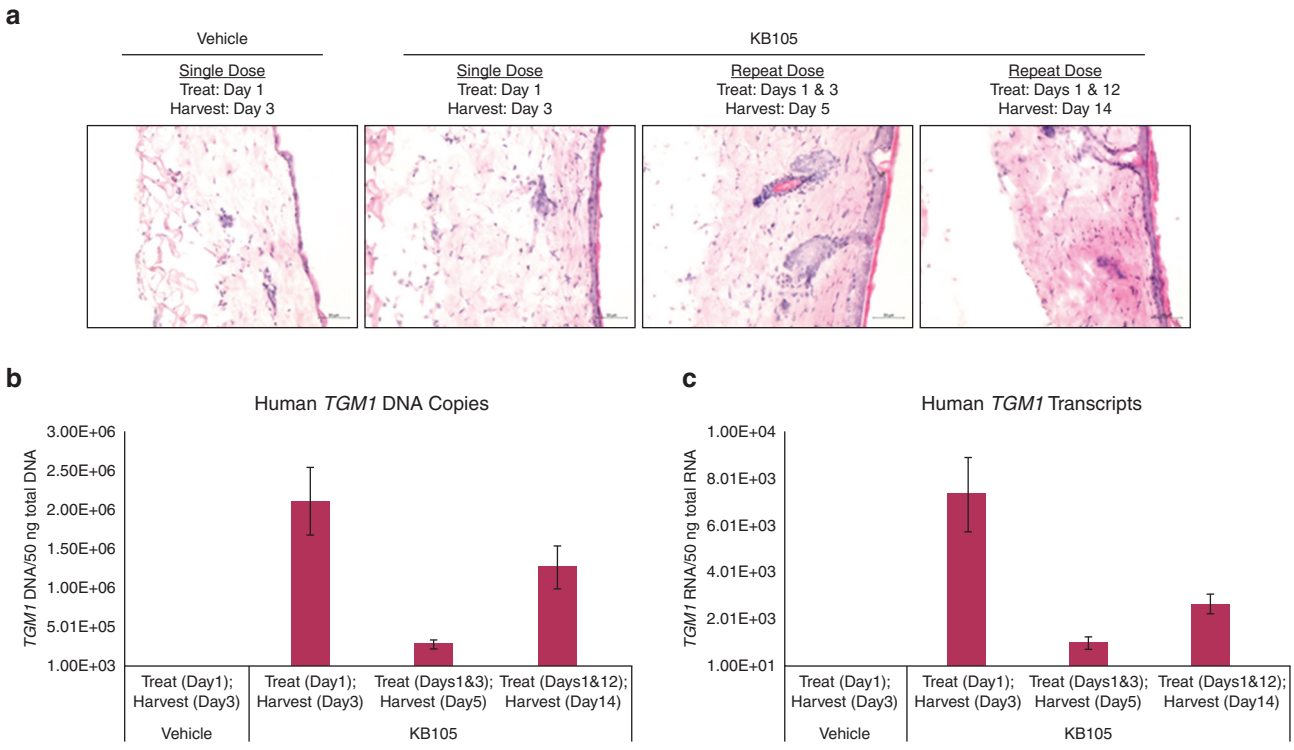

Figure 3. In vivo pharmacokinetics of KB105 on single and repeat topical delivery to BALB/c mice. (**a**) H&E-stained skin biopsies taken from BALB/c mice treated and harvested at the indicated timepoints after a single or repeat topical dose of either KB105 or negative control (vehicle). (**b**) Detection of human *TGM1* DNA copies in skin biopsies taken from BALB/c mice treated and harvested at the indicated timepoints after a single or repeat topical dose of either KB105 or negative control (vehicle). (**c**) Detection of human *TGM1* transcripts in skin biopsies taken from BALB/c mice treated and harvested at the indicated timepoints after a single or repeat topical dose of either KB105 or negative control (vehicle). For each vehicle control condition in the qPCR and QRT-PCR analysis, data are presented as the average of two tissue samples (two replicates tested per tissue sample) ± SEM; for each KB105 condition, data are presented as the average of four or six tissue samples (two replicates tested per tissue sample) ± SEM. (**d**) Representative IF images of human TGM1 and mouse loricrin protein colocalization in skin biopsies taken from BALB/c mice treated and harvested at the indicated timepoints after a single or repeat topical dose of either KB105 or negative control (vehicle). DAPI staining was used to visualize the nuclei. Bar = 50 μm. IF, immunofluorescence; QRT-PCR, quantitative real-time RT-PCR.

of the vehicle specifically used for these six mice. Detection of high levels of KB105 in group 2 mice was generally limited to the dose site, with no pronounced accumulation of the vector in other analyzed tissues (Supplementary Table S1). Vector persistence was minimal, as indicated by low-to-negative detection of vector copies obtained in the samples analyzed from recovery-phase mice.

DISCUSSION

Reliable delivery of functional TGM1 to human KCs is the paramount feature required of any gene therapy vector used for correcting the CE defect in patients with TGM1-deficient ARCI. In vitro, KB105 was evaluated for transduction efficiency and effector expression in cell-based assays using both immortalized and primary TGM1-deficient patient with ARCI-derived KCs. KB105 reproducibly infected relevant human KCs with high efficiency, capably rescued TGM1 protein expression, and restored functional TGM1 enzymatic activity in these otherwise TGM1-deficient patient cells.

Subsequent in vivo studies demonstrated successful dose-dependent vector transduction and subsequent TGM1 expression in relevant tissues of immunocompetent mice after topical application of KB105. The IF data indicated that the exogenously expressed human TGM1 colocalized with a native TGM1 substrate, loricrin, in the mouse epidermis, signifying proper targeting of and transgene delivery to the stratum granulosum. KB105 was also found to rapidly transduce the skin, with detectable vector genomes, *TGM1* transcripts, and TGM1 protein observable as early as 2 hours after administration.

A feasibility study of repeated topical administration using multiple dosing intervals indicated that KB105 efficiently transduced the skin and expressed its encoded human transgene at comparable levels after a first and subsequent topical treatment, irrespective of the length of delay between the treatments. Skin histology showed that KB105 was well-tolerated, even after repeated administration or when used at high dosages. Finally, Good Laboratory Practice biodistribution and toxicity data indicated that KB105 can be safely and repeatedly administered to the skin without systemic vector exposure. Taken together, these data provide strong support for the safe and effective recurrent use of topical KB105 for the transient and repeated delivery of human TGM1.

No prior gene therapies for ARCI have proceeded to clinical trials in the United States. However, several research groups have explored the methods of targeted TGM1 delivery to address the diseased phenotype in KCs lacking functional TGM1. These include both virus-mediated gene delivery approaches (Choate et al., 1996) and protein therapy

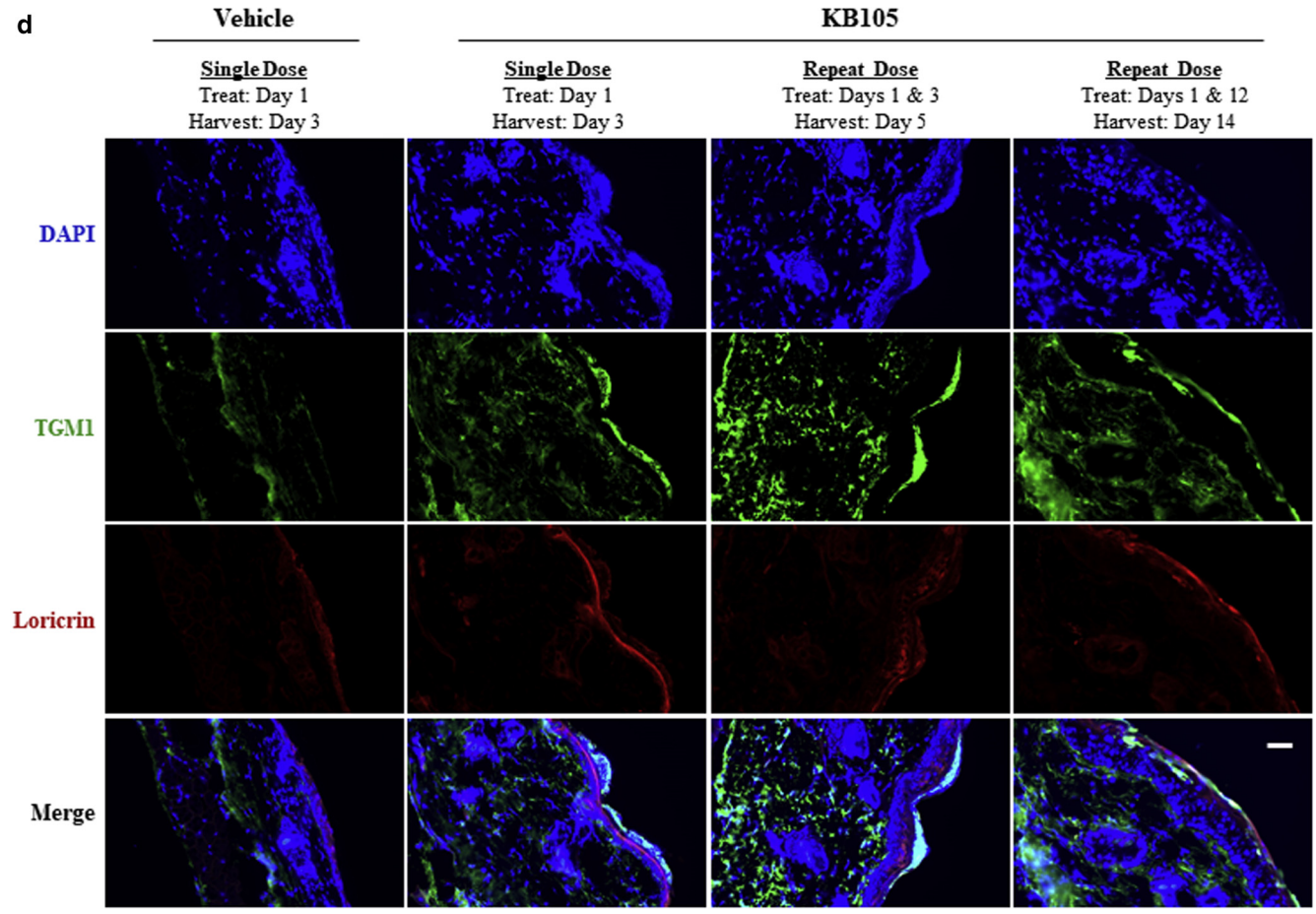

Figure 3. (*Continued*)

employing liposomally delivered purified recombinant TGM1 (Aufenvenne et al., 2013). Although successful in achieving durable correction of key disease features in the preclinical setting, neither of these approaches has moved into the clinic. These therapeutic modalities may suffer from significant challenges, including biological safety concerns and problems with upscale production and purification under the current Good Manufacturing Practice conditions. In the specific case of ex vivo cell therapies, high costs, long wait times, and the inherently invasive nature of the approach limit clinical applications. Given the lack of corrective options for patients suffering from ARCI, paired with the potential issues with prior TGM1 enzyme replacement approaches taken by others in the preclinical setting, there is thus a significant need for a localized, noninvasive, scalable gene therapy product based on a platform with a proven safety record in humans.

To this end, we have developed KB105, a ready-to-use gene therapy vector that is engineered to deliver functional human *TGM1* genes directly to the skin. Administering KB105 topically offers the potential for improved efficacy and reduced toxicity by delivering an increased vector concentration to the intent-to-treat site while reducing systemic exposure. Herpes simplex virus type 1 has a natural tropism to the outermost layer of the skin epithelium and can penetrate skin cells more efficiently than other viral vectors. Nonintegrating vectors such as herpes simplex virus type 1 do not insert themselves into the host's genome and thus do not disrupt the function of any host genes or present the cancer-causing risks associated with such disruption (e.g., as compared with retrovirus-mediated approaches of TGM1 replacement). In addition, the herpes simplex virus type 1 backbone from which KB105 is derived is being evaluated in humans and is the subject of a planned phase III clinical trial of our lead product candidate beremagene geperpavec. Of

Table 1. Design of the GLP Repeat-Dose Biodistribution and Toxicity Study

Group No.	No. of Animals[1] Male	No. of Animals[1] Female	Dose Level (PFU/Application)
1 (Vehicle control)[2]	18	18	0
2 (KB105)	18	18	1.07×10^9

Abbreviations; GLP, Good Laboratory Practice; No., number; PFU, plaque-forming unit.
[1]Mice designated for interim necropsy (six animals per sex per group) were euthanized on day 3 of the dosing phase. Mice designated for terminal necropsy (six animals per sex per group) were euthanized on day 30 of the dosing phase. All the remaining surviving mice underwent a 33-day recovery phase after the completion of dose administration and were euthanized on day 34 of the recovery phase (day 63 of the dosing phase).
[2]Group 1 was administered vehicle control formulated in gel excipient only.

the subjects repeatedly administered beremagene geperpavec through topical application, the intended route of administration for KB105, none have exhibited any signs of immunogenicity. No serious adverse events or drug-related adverse events have been reported to date, demonstrating the safety of the underlying vector platform.

The results from the studies described in this paper support KB105 as a potentially safe and effective treatment for TGM1-deficient ARCI. As such, we believe our therapeutic approach to molecularly correct TGM1 deficiency in patients with ARCI through topical application of KB105 presents an opportunity for safe, noninvasive treatment of this debilitating disease.

MATERIALS AND METHODS

Additional materials and methods can be found in the Supplementary Materials.

Cell culture

Cells were cultured at 37 °C in 5% carbon dioxide in the Cascade Biologics EpiLife medium (Gibco, Gaithersburg, MD). For qPCR, quantitative real-time RT-PCR, and western blot analysis, cells were grown in six-well dishes; cells were grown in eight-well chamber slides for IF and 96-well plates for the MTS assay (Abcam, Cambridge, MA).

In vitro virus infections

MOI was calculated from the virus titer and target cell number. The appropriate volume of virus stock was diluted in cell culture medium and incubated with target cells for 1 hour at 37 °C. Fresh medium was then added, and cells were grown at 37 °C in 5% carbon dioxide until harvest. For high-calcium cell culture medium, calcium chloride (final calcium ion concentration [1.8 mM]) was supplemented to the medium at the time of infection.

TGM1 activity assay

Slides were fixed in −20 °C acetone, washed three times with PBS, and blocked with 1% BSA and/or Tris-hydrogen chloride (pH 7.5). The slides were washed with PBS, blocked with Avidin-Biotin-Block solution (Life Technologies, Carlsbad, CA), and again washed with PBS. Transglutaminase 2 inhibitor (Zedira, Darmstadt, Germany) was incubated on the slides for 30 minutes at 37 °C in Tris-hydrogen chloride (pH 7.5) with 5 mM calcium chloride. The inhibitor was removed and KC transglutaminase 1–substrate peptide K5 (Zedira) was incubated with the slides for 2 hours at 37 °C. After the incubation, 25 mM EDTA was added to the slides to inhibit the reaction, the slides were washed three times with PBS, and Alexa Fluor 488–conjugated streptavidin avidin (Life Technologies, Carlsbad, CA) was added for 30 minutes at room temperature. Slides were washed with PBS, and background autofluorescence was darkened by treatment with 0.1% Sudan Black. Slides were then mounted with VectaShield HardSet (Vector Laboratories, Burlingame, CA) with DAPI.

Mice

All procedures followed applicable animal welfare acts and were approved by the Institutional Animal Care and Use Committee at Hilltop Lab Animals (Scottsdale, PA).

In vivo application of KB105 or vehicle control

Before the test article administration, the dorsal skin of each mouse was clipped free of fur, and depilatory cream was applied. After hair removal, portions of the dorsal skin were permeabilized using either tape stripping or acetone administration, as described previously (Ekanayake-Mudiyanselage et al., 1998).

To contain the topical formulation within the treatment area, a well was created from cut and autoclave-sterilized tops of 1.5 ml microcentrifuge tubes, and the cut sides of the lids were covered with OPSITE transparent adhesive dressing (Smith & Nephew, Andover, MA). The covered wells were adhered to the skin using surgical glue with the lid side down. A total of 120 μl of active or vehicle control test article formulated in a proprietary gel carrier (100 μl test article + 20 μl methylcellulose gel) was applied to the treatment site by injecting the formulation through the OPSITE dressing.

Tissue collection

The mice were killed, and each treatment site was biopsied using an 8-mm punch. Half of each skin biopsy was saved for qPCR and/or quantitative real-time RT-PCR analyses by quick freezing in liquid nitrogen, whereas the other half was embedded in optimal cutting temperature compound and cryopreserved for IF staining.

Data availability statement

No datasets are related to this article.

ORCIDs

John C. Freedman: http://orcid.org/0000-0002-8779-2914
Trevor J. Parry: http://orcid.org/0000-0002-9030-5275
Peipei Zhang: http://orcid.org/0000-0003-0918-0610
Avijit Majumdar: http://orcid.org/0000-0001-5035-5860
Suma Krishnan: http://orcid.org/0000-0003-2163-0194
Lauren K. Regula: http://orcid.org/0000-0002-0242-155X
Mark O'Malley: http://orcid.org/0000-0002-5463-977X
Sarah Coghlan: http://orcid.org/0000-0002-3550-508X
S.D. Yogesha: http://orcid.org/0000-0002-6588-3911
Sureshkumar Ramasamy: http://orcid.org/0000-0002-2088-8065
Pooja Agarwal: http://orcid.org/0000-0002-8922-8145

CONFLICT OF INTEREST

The authors of this manuscript are employees of and have a financial and/or equity interest in Krystal Biotech, Inc, which is developing commercial products related to the research being reported. Krystal Biotech, Inc is also pursuing one or more patents related to these technologies.

ACKNOWLEDGMENTS

We thank Keith Choate for kindly providing us with the TGM1-deficient autosomal recessive congenital ichthyosis keratinocytes and Jennifer Patton for her contributions to our mouse studies. We also thank A. Collin and B. Popovic for their contributions.

AUTHOR CONTRIBUTIONS

Conceptualization: SK, PA, JCF; Data Curation: JCF, PZ, AM; Formal Analysis: JCF, PZ, AM, TJP, SK, PA; Investigation: JCF, PZ, AM, TJP, SK, PA; Methodology: JCF, PZ, AM, TJP, SK, PA; Resources: JCF, PZ, AM, LKR, MOM, SC, SDY, SR; Supervision: SK, PA; Writing - Original Draft Preparation: JCF, TJP; Writing - Review and Editing: JCF, TJP, PZ, AM, SK, LKR, MOM, SC, SDY, SR, PA

SUPPLEMENTARY MATERIAL

Supplementary material is linked to the online version of the paper at www.jidonline.org, and at https://doi.org/10.1016/j.jid.2020.07.035.

REFERENCES

Aufenvenne K, Larcher F, Hausser I, Duarte B, Oji V, Nikolenko H, et al. Topical enzyme-replacement therapy restores transglutaminase 1 activity and corrects architecture of transglutaminase-1-deficient skin grafts. Am J Hum Genet 2013;93:620–30.

Candi E, Schmidt R, Melino G. The cornified envelope: a model of cell death in the skin. Nat Rev Mol Cell Biol 2005;6:328–40.

Choate KA, Medalie DA, Morgan JR, Khavari PA. Corrective gene transfer in the human skin disorder lamellar ichthyosis. Nat Med 1996;2:1263–7.

Chung M, Pittenger J, Tobin S, Chung A, Desai N. Expedient treatment of a collodion baby Case Rep Dermatol Med 2011;2011:803782.

Ekanayake-Mudiyanselage S, Aschauer H, Schmook FP, Jensen JM, Meingassner JG, Proksch E. Expression of epidermal keratins and the cornified envelope protein involucrin is influenced by permeability barrier disruption. J Invest Dermatol 1998;111:517–23.

Farasat S, Wei MH, Herman M, Liewehr DJ, Steinberg SM, Bale SJ, et al. Novel transglutaminase-1 mutations and genotype-phenotype investigations of 104 patients with autosomal recessive congenital ichthyosis in the USA. J Med Genet 2009;46:103–11.

Gånemo A, Pigg M, Virtanen M, Kukk T, Raudsepp H, Rossman-Ringdahl I, et al. Autosomal recessive congenital ichthyosis in Sweden and Estonia: clinical, genetic and ultrastructural findings in eighty-three patients. Acta Derm Venereol 2003;83:24–30.

Herman ML, Farasat S, Steinbach PJ, Wei MH, Toure O, Fleckman P, et al. Transglutaminase-1 gene mutations in autosomal recessive congenital ichthyosis: summary of mutations (including 23 novel) and modeling of TGase-1. Hum Mutat 2009;30:537–47.

Matsuki M, Yamashita F, Ishida-Yamamoto A, Yamada K, Kinoshita C, Fushiki S, et al. Defective stratum corneum and early neonatal death in mice lacking the gene for transglutaminase 1 (keratinocyte transglutaminase). Proc Natl Acad Sci USA 1998;95:1044–9.

Pigg M, Gedde-Dahl T Jr, Cox D, Hausser I, Anton-Lamprecht I, Dahl N. Strong founder effect for a transglutaminase 1 gene mutation in lamellar ichthyosis and congenital ichthyosiform erythroderma from Norway. Eur J Hum Genet 1998;6:589–96.

Rissmann R, Oudshoorn MH, Hennink WE, Ponec M, Bouwstra JA. Skin barrier disruption by acetone: observations in a hairless mouse skin model. Arch Dermatol Res 2009;301:609–13.

Rodríguez-Pazos L, Ginarte M, Vega A, Toribio J. Autosomal recessive congenital ichthyosis. Actas Dermosifiliogr 2013;104:270–84.

Orphanet. Prevalence of rare diseases: bibliographic data, Orphanet report series, rare diseases collection, number 1: diseases listed in alphabetical order. https://www.orpha.net/orphacom/cahiers/docs/GB/Prevalence_of_rare_diseases_by_alphabetical_list.pdf; 2020 (accessed 14 July 2020).

Yang CS, Pomerantz H, Mannava KA, Corwin J, Weinstock MA, Fleckman P, et al. Comparing histopathology from patients with X-linked recessive ichthyosis and autosomal recessive congenital ichthyosis with transglutaminase 1 mutation: a report from the National Registry for Ichthyosis and Related Skin Disorders. J Am Acad Dermatol 2016;74:1008–10.e2.

SUPPLEMENTARY MATERIALS AND METHODS

Cell culture

Deidentified patients with TGM1-deficient autosomal recessive congenital ichthyosis cells were obtained from previously isolated skin biopsies harvested at Yale University (New Haven, CT) as part of routine surgical or diagnostic procedures (with Institutional Review Board approval), and a subset was immortalized. Informed written consent was obtained from each patient or, in the case of children, from the parent or legal guardian.

qPCR and/or quantitative real-time RT-PCR

For nucleic analysis in the in vitro studies, cells were plated in six-well plates to achieve 85–90% confluency on the following day. After viral infection, cells were resuspended in 350 μl of RLT buffer containing dithiothreitol (Qiagen, Germantown, MD) and homogenized by passing through a QiaShredder (Qiagen) column according to the manufacturer's instructions. Alternatively, for nucleic acid analyses in the in vivo studies, quick-frozen tissue biopsy halves were resuspended in 350 μl RLT buffer containing *dithiothreitol* and sonicated three times at 25% amplitude, with intermittent incubations for 1 minute on ice. DNA and RNA were isolated using the AllPrep DNA/RNA Mini Kit (Qiagen). A total of 25 ng or 50 ng of DNA or RNA per reaction were used in TaqMan Fast Advanced Master Mix for qPCR (Applied Biosystems, Carlsbad, CA) or 1-Step RT-qPCR ToughMix (Quantabio, Beverly, MA) for quantitative real-time RT-PCR. A ×20 primer and/or probe mix containing 45 nmoles of forward (5′-GACAATTCCCATGGCCAGTA-3′) and reverse (5′-CAGATGGCTGGCAACTAGAA-3′) primers and 12.5 nmoles probe (56-FAM/ACGGGATCC/ZEN/GCGGTTTAAACTCAA/3IABkFQ/) was used. All samples were run in duplicate, and the copy number was determined using a standard curve derived from a dilution series of plasmid standard containing a known copy number of the *TGM1* coding sequence used to construct KB105.

Western blots

Cells were plated in six-well plates to achieve 85–90% confluency on the following day. After viral infection, cells were lysed in RIPA buffer and incubated with intermittent agitation for 20 minutes. At this time, benzonase (Millipore sigma, Burlington, MA) was added to each lysate for 10 minutes at room temperature and centrifuged at 4 °C for 5 minutes. The total protein concentration of the supernatant was determined using a Pierce MicroBCA assay (ThermoFisher, Waltham, MA), and the lysate was mixed with ×4 lithium dodecyl sulfate sample buffer containing 5% 2-mercaptoethanol. Before loading, samples were boiled for 5 minutes at 95 °C, allowed to cool to room temperature, and cleared by centrifugation. A total of 22.5 μg total protein was loaded into each well of a 4–20% Tris-Glycine gel (ThermoFisher). The gels were run at 200 V for 60 minutes and transferred to polyvinylidene difluoride (Millipore, Burlington, MA) at 45 V for 90–100 minutes. Blots were then blocked for 30 minutes in 5% milk and/or Tris-buffered saline before adding primary antibodies (rabbit anti-TGM1, catalog number [cat. no.] ab103814, Abcam, Cambridge, MA; rabbit anti-GAPDH, cat. no. Ab9485, Abcam) and incubating overnight at room temperature. Next, blots were incubated with IRDye 800CW-conjugated goat anti-rabbit IgG secondary antibody (LI-COR Biosciences, Lincoln, NE) for 1 hour at room temperature, washed three times with Tris-buffered saline for 5 minutes, and imaged directly on an LI-COR Biosciences Odyssey CLx Imaging System. The relative amount of TGM1 expression was determined using Image Studio Lite, version 5.2 (LI-COR Biosciences) by determining the TGM1 band intensity relative to GAPDH band intensity in each sample.

In vitro immunofluorescence

Cells were plated in eight-well chamber slides to achieve 85–90% confluency on the following day. After viral infection, the medium was aspirated from the slides, −20 °C methanol was added to each chamber, and the slide was incubated at −20 °C for 20 minutes. The methanol was then removed, the slides were washed three times with room temperature PBS, and the chamber apparatus was removed from the slide. Slides were blocked for 30 minutes at room temperature in 5% BSA and/or PBS and then treated with primary Ab for 2 hours at room temperature (rabbit anti-TGM1, cat. no. ab103814., Abcam). Slides were washed three times with PBS at room temperature, and Alexa Fluor-488–conjugated goat anti-rabbit IgG Ab (Invitrogen, Waltham, MA) was added for 1 hour at room temperature. Slides were again washed with PBS, the slides were aspirated thoroughly, and VectaShield HardSet (Vector Laboratories, Burlingame, CA) with DAPI was added. Slides were visualized on an ECHO Revolve fluorescence microscope (ECHO Labs, San Diego, CA).

Fluorescence intensity quantification

Fluorescence intensity was quantified from the raw images acquired from the in vitro immunofluorescence and in situ experiments using ImageJ software (National Institutes of Health, Bethesda, MD). Quantification was performed by calculating the average fluorescence intensity of two ×10 fields.

In vivo immunofluorescence

5-μm sections were taken from optimal cutting temperature compound–frozen tissue, mounted on slides, and air dried for up to 1 hour. The slides were then dipped in 100% methanol for 10 minutes at −20 °C and left to air dry. The methanol-fixed sections were rehydrated by washing three times in PBS (5 minutes each) at room temperature. A total of 3% hydrogen peroxide (VWR International, Radnor, PA) was applied to the rehydrated sections to block endogenous peroxidase activity, and the samples were incubated with Power Block solution (Biogenex Laboratories, Fremont, CA) for 10 minutes at room temperature in a humidified chamber. Excess blocking solution was removed, and the sections were stained with a drop of primary Ab (anti-human TGM1, cat. no. A042, Zedira, Darmstadt, Germany; anti-mouse loricrin, cat. no. ab85679, Abcam; anti-human/mouse integrin alpha-6, cat. no. 555734, BD Biosciences, San Jose, CA) prepared in an Ab-diluent buffer (30–50 μl primary Ab solution per section). The sections were incubated with the primary Ab for 16 hours at 4 °C or 1 hour at room temperature and washed three times in Tris-buffered saline + 0.025% Triton X-100 for 5 minutes at room temperature, and secondary Ab (Alexa

Fluor 488–conjugated anti-mouse, cat. no. A-11029, ThermoFisher; Alexa Fluor 594–conjugated anti-rabbit, cat. no. ab150080, Abcam; anti-rat IgG [H+L] cross adsorbed, Cyanine5, cat. no. A10525, ThermoFisher) was applied at a 1:200 dilution in an Ab-diluent buffer for 30 minutes at room temperature in a humidified chamber. Slides were once again washed three times with Tris-buffered saline + 0.025% Triton X-100, and the stained sections were mounted with mounting media (ProLongTM Gold Antifade Mountant with DAPI, ThermoFisher) and covered with a coverslip. The sections were imaged after dehydration (approximately 24 hours) using an ECHO Revolve fluorescence microscope.

MTS viability assay

Primary keratinocytes were seeded at the appropriate density in 96-well culture dishes and grown to 85−90% confluence overnight. The next day, monolayers were infected at the indicated multiplicity of infection. After 48 hours, cell viability was measured using an MTS assay as described by the manufacturer (Abcam). The percentage viability was calculated by normalizing to mock-treated cells (100% viability).

H&E staining

Five-micrometre sections were taken from cryopreserved tissue, mounted on slides, and air dried for up to 1 hour. The dried slides were rehydrated by soaking in double-distilled water for 2 minutes at room temperature. Sections were incubated in Hematoxylin Gill ×2 (VWR International) for 2 minutes at room temperature, dipped 2−3 times in acid alcohol, dipped 3−4 times in Blue in ammonia water, and incubated in eosin (Eosin Y Solution 1%, VWR International) for 2 minutes. Samples were rinsed 3−4 times with tap water between each step. The stained and rinsed sections were gradually dehydrated with ethanol by first rinsing twice with 95% ethanol for 2 minutes each and then twice with 100% ethanol for 2 minutes each. Sections were cleared through three rinses with Histo-Clear (VWR International) for 2 minutes each, mounted with mounting media (Permount Mounting Medium; Fisher Scientific, Pittsburgh, PA), and covered with a coverslip. The sections were imaged approximately 24 hours after dehydration using a bright-field microscope.

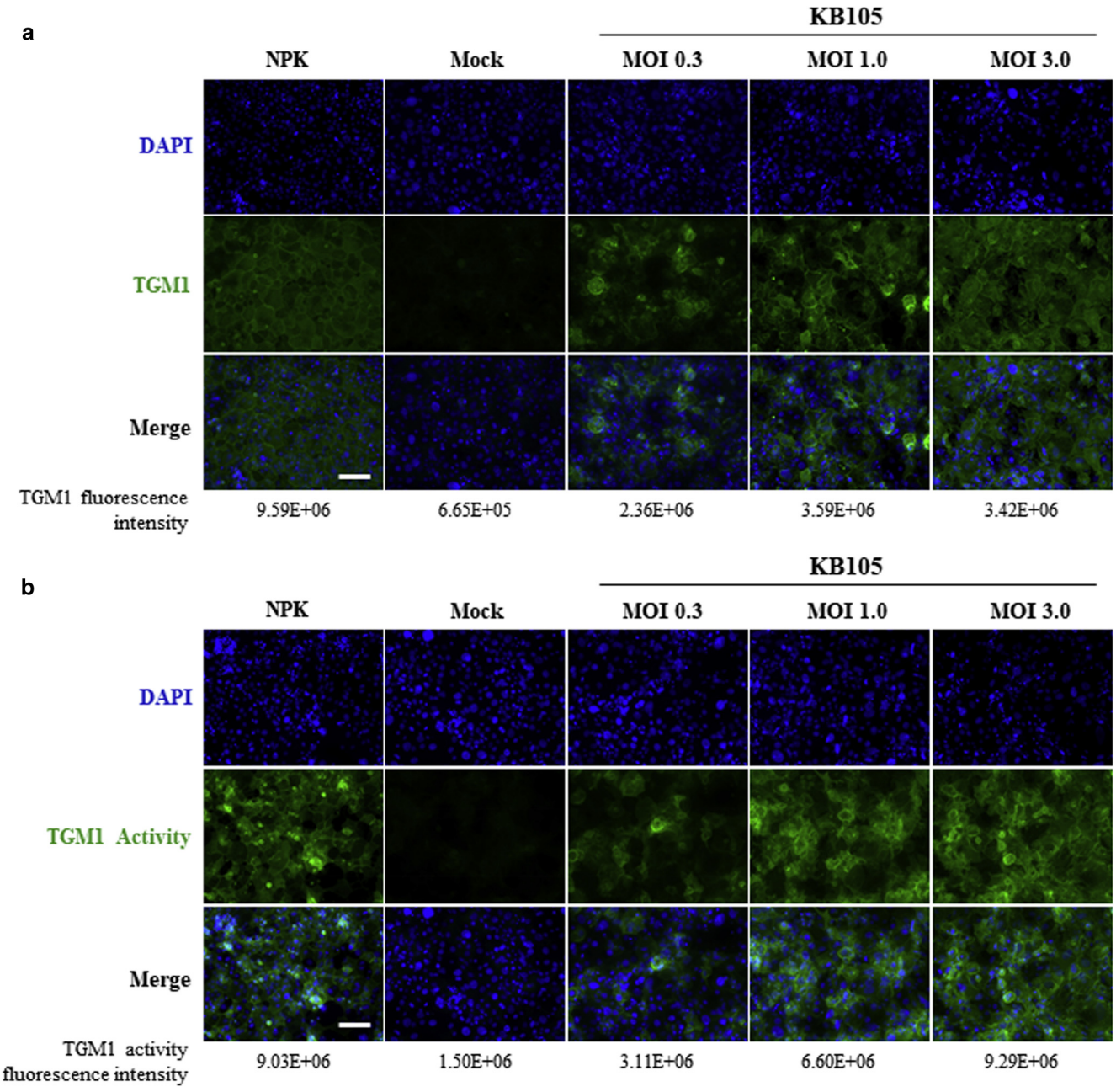

Supplementary Figure S1. In vitro assessment of KB105 in immortalized TGM1-deficient human ARCI KCs grown in a high-calcium cell culture medium. (**a**) Representative IF images of human TGM1 protein expression on KB105 infection of immortalized KCs. (**b**) Representative IF images of KB105-dependent TGM1 enzymatic activity in immortalized KCs. Uninfected (mock) cells were used as negative controls; NPKs were used as positive controls. DAPI staining was used to visualize the nuclei. Quantification of fluorescence intensities is provided for each condition. Bar = 130 μm. ARCI, autosomal recessive congenital ichthyosis; IF, immunofluorescence; KC, keratinocyte; MOI, multiplicity of infection; NPK, normal primary KC.

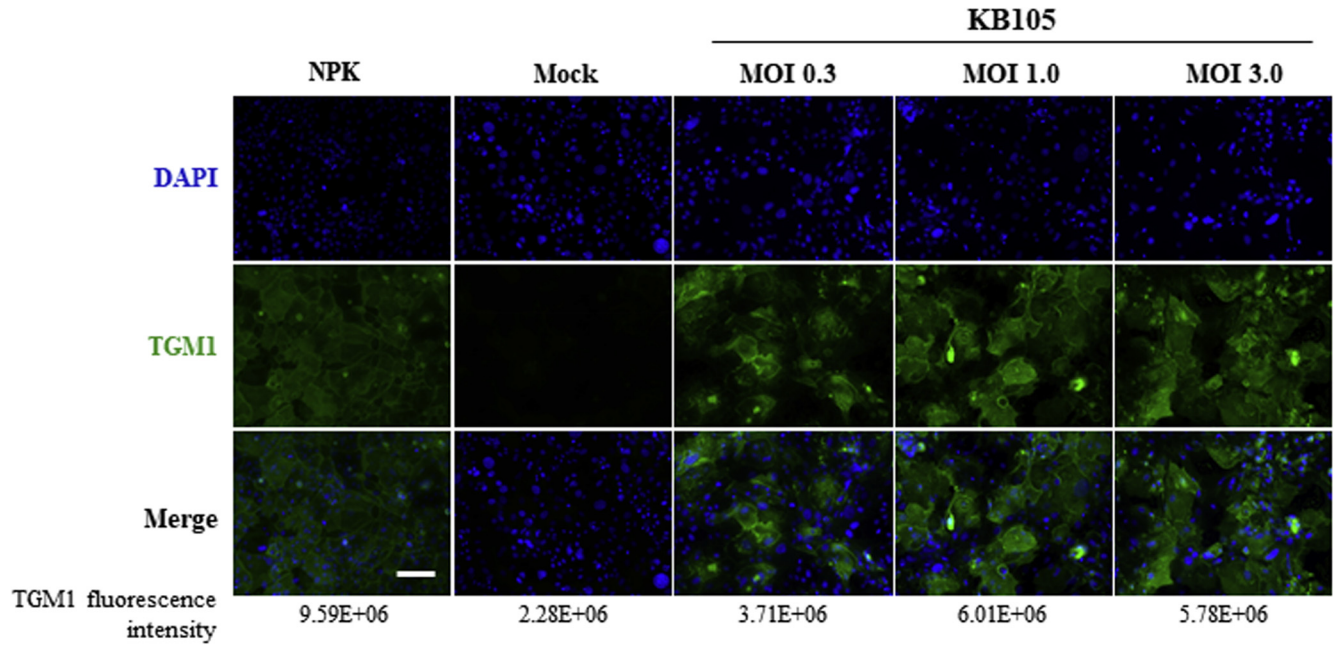

Supplementary Figure S2. In vitro assessment of KB105 in primary TGM1-deficient human ARCI KCs grown in a high-calcium cell culture medium. Representative IF images of human TGM1 protein expression on KB105 infection of primary KCs. Uninfected (mock) cells were used as negative controls; NPKs were used as positive controls. DAPI staining was used to visualize the nuclei. Quantification of fluorescence intensities is provided for each condition. Bar = 130 μm. ARCI, autosomal recessive congenital ichthyosis; IF, immunofluorescence; KC, keratinocyte; MOI, multiplicity of infection; NPK, normal primary KC.

Supplementary Figure S3. Viability assessments after KB105 infection of primary TGM1-deficient human ARCI KCs grown in low- and high- calcium cell culture medium. (**a**) Representative bright-field images of primary KCs, grown in a low- or high-calcium cell culture medium, at 48 hours after infection with KB105 at the indicated MOIs. Uninfected (mock) cells were used as a negative control. (**b**) Viability assessment of KB105-infected primary ARCI patient KCs at 48 hours after infection as determined by MTS assay. For each condition, data are presented as the average of three separate experiments (with triplicate wells) ± SEM. Bar = 370 μm. ARCI, autosomal recessive congenital ichthyosis; Ca^{2+}, calcium ion; KC, keratinocyte; MOI, multiplicity of infection.

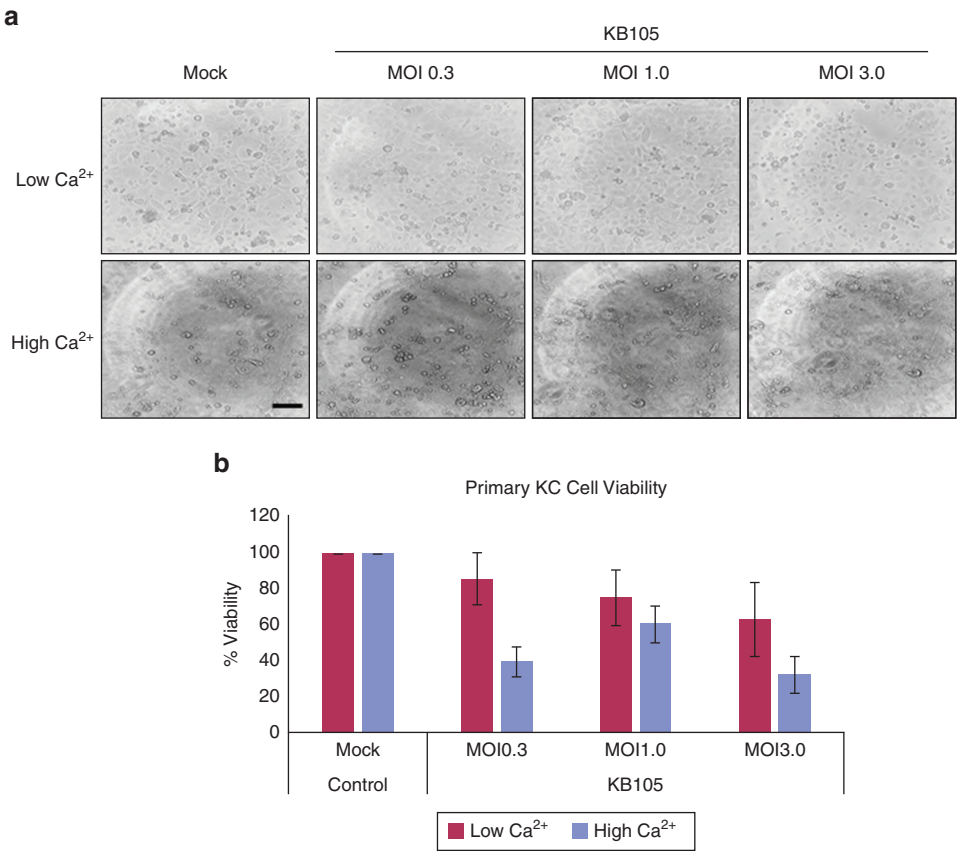

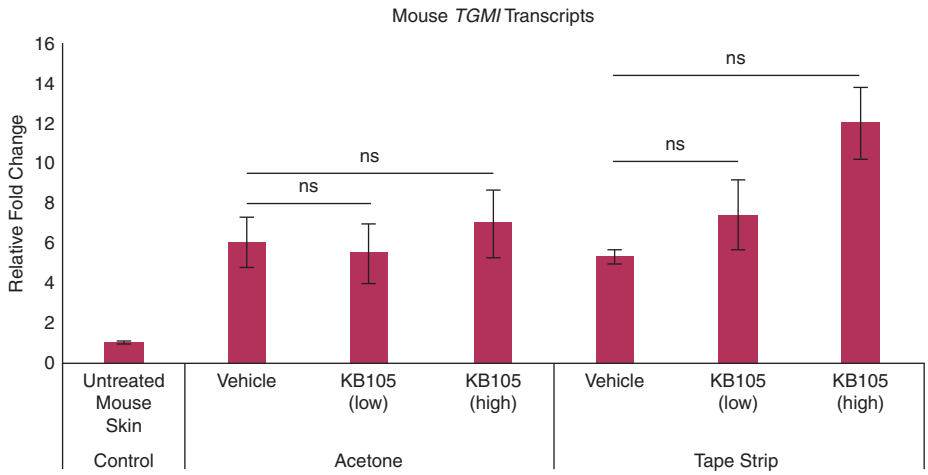

Supplementary Figure S4. In vivo evaluation of mouse *TGM1* transcription on KB105 infection through multiple routes of topical delivery to BALB/c mice. Fold change of mouse *TGM1* RNA copies in skin biopsies harvested at 48 hours after permeabilization by tape stripping or acetone treatment and application of KB105 (low or high dose) or vehicle alone relative to untreated control skin, as assessed by QRT-PCR. For each vehicle condition, data are presented as the average of two tissue samples (two replicates tested per tissue sample) ± SEM; for each KB105 condition, data are presented as the average of four tissue samples (two replicates tested per tissue sample) ± SEM ($P > 0.05$), as determined by two-tailed Student's *t*-test. Bar = 50 μm. ns, not significant; QRT-PCR, quantitative RT-PCR.

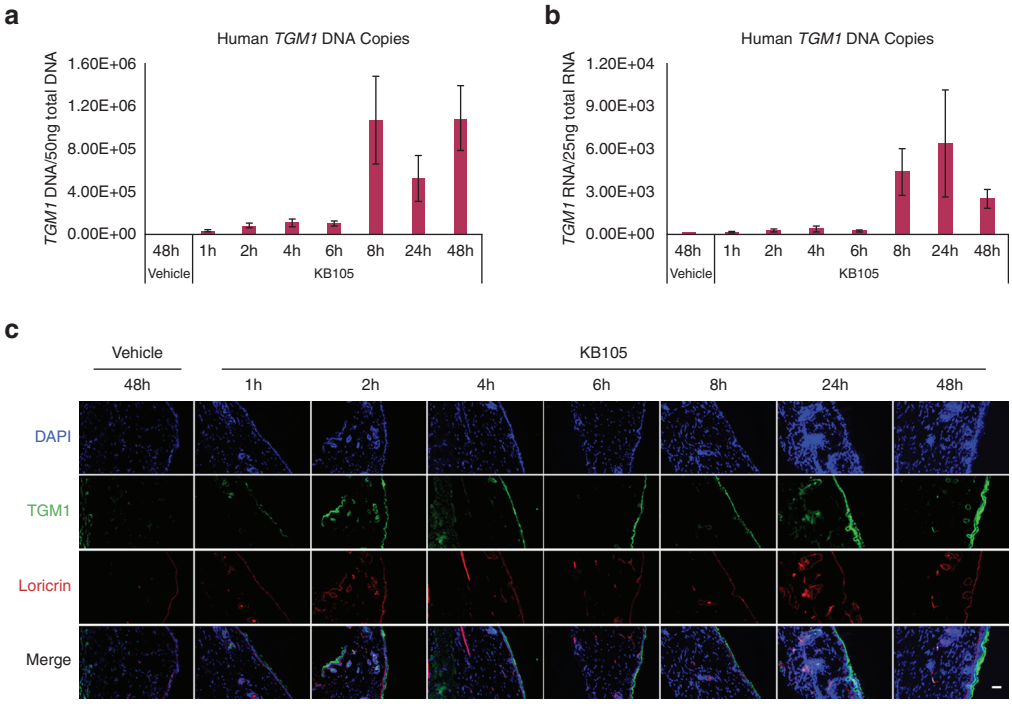

Supplementary Figure S5. In vivo short-term pharmacokinetics of KB105 on topical delivery to BALB/c mice. (**a**) Detection of human *TGM1* DNA copies in skin biopsies harvested at the indicated timepoints from BALB/c mice treated topically with either KB105 or negative control (vehicle). (**b**) Detection of human *TGM1* transcripts in skin biopsies harvested at the indicated timepoints from BALB/c mice treated topically with either KB105 or negative control (vehicle). For each vehicle control condition in the qPCR and QRT-PCR analysis, data are presented as the average of two tissue samples (two replicates tested per tissue sample) ± SEM; for each KB105 condition, data are presented as the average of four tissue samples (two replicates tested per tissue sample) ± SEM. (**c**) Representative IF images of human TGM1 and mouse loricrin protein localization in mouse skin biopsies harvested at the indicated timepoints from BALB/c mice treated topically with either KB105 or negative control (vehicle). DAPI staining was used to visualize the nuclei. Bar = 50 μm. h, hour; IF, immunofluorescence; QRT-PCR, quantitative real-time RT-PCR.

Supplementary Table S1. Average Vector Biodistribution in Selected Tissues Harvested during the GLP Repeat-Dose Biodistribution and Toxicity Study, as Assessed by qPCR Analysis

	Day 3 (Interim)				Day 30 (Terminal)				Day 63 (Recovery)			
	Vehicle		KB105		Vehicle		KB105		Vehicle		KB105	
Tissue	M	F	M	F	M	F	M	F	M	F	M	F
Blood	BLOD	BLOD	BLOD	BLOD	BLOD	BLOD	BLOD	46 (±46)	NA	NA	NA	NA
Bone marrow (femur)	BLOD	BLOD	101,868 (±101,815)	571 (±300)	BLOD	BLOD	BLOD	BLOD	NA	NA	NA	NA
Brain, frontal lobe	BLOD	BLOD	BLOD	BLOD	BLOD	BLOD	BLOD	BLOD	NA	NA	NA	NA
Dose site	BLOD	2,853 (±682)	22,685,102 (±8,655,848)	49,566,540 (±13,628,864)	BLOD	BLOD	13,695,879 (±6,694,173)	11,595,528 (±8,494,385)	BLOD	BLOD	22 (±15)	10 (±10)
Heart, apex	BLOD	BLOD	28 (±28)	BLOD	BLOD	BLOD	BLOD	BLOD	NA	NA	NA	NA
Kidney, left	BLOD	BLOD	BLOD	BLOD	BLOD	BLOD	63 (±63)	BLOD	NA	NA	NA	NA
Liver, left lateral lobe	BLOD	BLOD	BLOD	BLOD	BLOD	BLOD	BLOD	9 (±9)	NA	NA	NA	NA
Lung, right lobe, caudal	BLOD	BLOD	BLOD	BLOD	BLOD	BLOD	BLOD	BLOD	NA	NA	NA	NA
Lymph node, axillary	BLOD	BLOD	132 (±132)	73 (±73)	BLOD	BLOD	BLOD	BLOD	NA	NA	NA	NA
Lymph node, inguinal	BLOD	BLOD	28 (±28)	166 (±166)	BLOD	BLOD	122 (±44)	BLOD	NA	NA	NA	NA
Ovary, left	NA	BLOD	NA	BLOD	NA	BLOD	NA	BLOD	NA	NA	NA	NA
Ovary, right	NA	NA	NA	NA	NA	BLOD	NA	BLOD	NA	NA	NA	NA
Spleen	BLOD	BLOD	BLOD	BLOD	BLOD	BLOD	BLOD	BLOD	NA	NA	NA	NA
Testis, left	BLOD	NA	BLOD	NA	BLOD	NA	BLOD	NA	NA	NA	NA	NA

Abbreviations: BLOD, below limit of detection; F, female; GLP, Good Laboratory Practice; M, male; NA, not applicable.
Data are presented as the average number of detected vector genome copies (±SEM).